Measurements of criticality in the Olami-Feder-Christensen model

G. Miller and C. J. Boulter
Department of Mathematics, Heriot-Watt University, Edinburgh EH14 4AS, United Kingdom
(Received 17 April 2002; published 24 July 2002)

The Olami-Feder-Christensen model is a simple lattice based cellular automaton model introduced as a prototype to study self-organization in systems with a continuous state variable. Despite its simplicity there remains controversy over whether the system is truly critical in the nonconservative regime. Here we address this issue by introducing the layer branching rate, which measures how contributions to the system branching rate vary across the lattice. By considering this quantity for layers far from the edges of the finite-sized lattices, we find that the model is only critical in the conservative limit, but that previous studies have underestimated the system branching rate in the nonconservative case. We further derive expressions for the branching rate in systems where the state variable across the lattice is described by a uniform distribution, in order to determine the effect of self-organization upon the level of criticality. We find that organization raises the branching rate in the nearest-neighbor case, but in contrast lowers the level of criticality in a random-neighbor model.

DOI: 10.1103/PhysRevE.66.016123 PACS number(s): 05.65.+b, 45.70.Ht, 05.45.Ra

I. INTRODUCTION

The concept of self-organized criticality (SOC) [1,2] was introduced by Bak, Tang, and Wiesenfeld (BTW) [3] in 1987 in order to explain the presence of scale invariance in a range of naturally occurring systems. The BTW model consists of a lattice with a number of sand grains at each site. The model is driven by the random addition of sand, and relaxes via a sequence of avalanches. As this process is repeated the model evolves to a critical state where characteristic scales in space and time are lost. At each stage the number of grains of sand is conserved (except at the system boundaries) and it has been shown that this conservation is essential for criticality in the BTW model [4].

In many physical systems displaying apparent scale invariance there is some level of dissipation. For example, one may consider earthquakes or landslide dynamics where the appropriate dynamical variables are not necessarily conserved; thus one must go beyond the BTW model. In an attempt to examine the effect of nonconservation on criticality Olami, Feder, and Christensen (OFC) [5] introduced a model motivated by the Burridge-Knopoff spring-block description of earthquake dynamics [6]. The model is described in detail in Sec. II and should be viewed as a toy model for understanding some generic features of self-organization rather than a realistic model of a particular physical process, playing much the same role as the Ising model does in statistical mechanics.

Within the OFC model there is a conservation parameter α. When $\alpha=0.25$ the dynamic variables are conserved during the avalanche process, whereas when $\alpha<0.25$ there is some level of dissipation which grows as α is reduced. There exists a critical value of the conservation parameter $0<\alpha_c \leqslant 0.25$ such that the model displays genuine critical behavior for $\alpha \geqslant \alpha_c$ and is noncritical for $\alpha<\alpha_c$. For a random-neighbor version of the model it has been analytically established that the system is never critical in the nonconservative regime [7,8]. Within the nearest-neighbor version of the model, determining the value of α_c has proved controversial and this is one of the issues that we focus on in this paper. In particular, in Sec. III, we introduce layer branching rates for the OFC model to provide a more controlled method for extrapolating results to the infinite-lattice limit. In this way we predict that $\alpha_c=0.25$ so that one only finds critical behavior in the conservative limit. However, our method predicts that for $\alpha<\alpha_c$ the OFC model is nearer criticality than many previous estimates have suggested.

In Sec. IV we introduce control cases for both the random- and nearest-neighbor versions of the OFC model in order to examine how well the models organize themselves. For the nearest-neighbor model we find that, although the model is only critical in the conservative regime, the organizational process is a positive one, resulting in near criticality for a range of α values. In contrast, self-organization in the random-neighbor model lowers criticality with respect to the control case, making this a poor model whenever $\alpha<0.25$. Finally, in Sec. V we summarize our results and highlight the main conclusions of our study.

II. THE OLAMI-FEDER-CHRISTENSEN MODEL

The OFC model [5] is a lattice based model which can be defined in arbitrary space dimensions [1]. For the purposes of this paper we concentrate on the two-dimensional case in which each node (i,j) on a square lattice is associated with a continuous state variable or energy u_{ij}. Initially the energies are assigned random values in an interval $[0,1)$ say; the upper limit on this interval coincides with the "threshold" defined below and can be fixed to unity without loss of generality. The system is then slowly driven in such a way that the energy at all the sites increases uniformly until one of the sites reaches the threshold value $u_{ij}=1$ and is termed supercritical. When this happens an avalanche occurs at a time scale much quicker than the driving speed. The supercritical site relaxes according to

$$u_{ij} \rightarrow 0, \tag{2.1}$$

with its energy distributed to (typically) four neighbors u_{nbrs}, using the rule

$$u_{\mathrm{nbrs}} \rightarrow u_{\mathrm{nbrs}} + \alpha u_{ij}, \tag{2.2}$$

where α is the conservation parameter discussed in Sec. I. If any of the neighboring sites become supercritical (i.e., $u_{\mathrm{nbrs}} \geqslant 1$) as a result of this process they also topple according to the same rules. The toppling process is non-Abelian and so if more than one site is supercritical either the sites must be toppled simultaneously, or a special sequential update must be employed [9]. The avalanche continues until all node values are below the threshold, at which stage the driving process proceeds until the next event is triggered. The two time scales involved in the dynamics of the model are motivated from physical behavior such as earthquakes, where stress builds up slowly between tectonic plates over years or decades (the driving phase), while the energy release of the earthquake (the toppling phase) occurs over seconds or minutes.

Within the model the parameter α measures the level of nonconservation in the system. If $\alpha = 0.25$ all of the energy of the toppling site is redistributed to its neighbors and so energy is conserved, while if $\alpha < 0.25$ it is not. Two distinct versions of the model are defined by the choice of neighboring sites to which energy is distributed. For the *nearest-neighbor (NN) OFC model* the sites adjacent to the toppling site are chosen. If the toppling site is on the edge of a lattice there are a reduced number of neighbors (two for a corner and three for an edge); thus the edges provide the only method of dissipation in the conservative case $\alpha = 0.25$. Further, the edges introduce an inhomogeneity into the system which prevents synchronization and is crucial if one is to observe SOC [10]. In a *random-neighbor (RN) OFC model* four sites are chosen at random to receive the toppling energy, with the assignment of neighbors changing at each update, thereby removing any spatial correlations in the system and preventing the possibility of synchronization. In the conservative limit one must include a dissipation mechanism to allow the system to relax to a stable state, which may be done by simulating the effect of boundaries via the number of neighbors chosen for each toppling site. For example, on a lattice of size $L \times L$, one could choose two neighbors (corner), three neighbors (edge), or four neighbors (bulk) with probabilities $4/L^2$, $4(L-2)/L^2$, and $(L-2)^2/L^2$, respectively.

The presence of a self-organized critical state is indicated by a power law distribution of a measured event, for example, the distribution of avalanche sizes in the OFC model. Thus, as a first attempt to identify the critical value α_c, which separates the critical and noncritical regimes as described in Sec. I, one may examine log-log plots of simulation data searching for straight line fits over several decades. On this basis Olami, Feder, and Christensen initially identified $\alpha_c^{\mathrm{NN}} \approx 0.05$ [5] for the nearest-neighbor OFC model. Larger scale simulations have indicated that the critical value is somewhat higher, with Grassberger predicting $\alpha_c^{\mathrm{NN}} \geqslant 0.18$ [10] and more recent work suggesting $\alpha_c^{\mathrm{NN}} \approx 0.25$ [11], indicating that the nearest-neighbor model is never critical in the nonconservative case. The primary difficulty in establishing a definitive result via this route has been the inability to simulate sufficiently large lattices. In the OFC model the system reaches an organized state only after a ''transient period'' which grows rapidly with lattice size, severely limiting the ability to simulate large lattices.

For the random-neighbor OFC model analytic progress has been possible using mean-field type calculations. Much of the formalism was developed by Lise and Jensen (LJ) [12], who used a very simplified approximation for the distribution of energies u_{ij} across the lattice to predict $\alpha_c^{\mathrm{RN}} = 2/9$. Using a more realistic energy distribution reveals that the model is only critical in the conservative limit so $\alpha_c^{\mathrm{RN}} = 0.25$ [7,8,13]. The LJ approach for the random-neighbor model involves an analysis of the branching rate, $\sigma(\alpha)$ say, which measures the average number of supercritical descendants generated when a single supercritical site topples. In the absence of an analytic solution for the nearest-neighbor OFC model, and given the limitations on the size of lattices that can be simulated discussed above, it has proved valuable to also numerically analyze the branching rate in the nearest-neighbor case.

In a simulation one simply counts the number of supercritical descendants generated when each supercritical ancestor topples. The number of descendants assigned to an ancestor may be noninteger, since a supercritical descendant that has originated from more than one neighboring ancestor has its contribution split evenly between those ancestors. Further, sites at the boundary may have their branching rate weighted according to the number of neighbors present in order to avoid artificially lowering σ in a finite-size system [11]. It is straightforward to establish that the branching rate $\sigma(\alpha,L)$ in a finite-size $(L \times L)$ system satisfies [14]

$$\sigma(\alpha,L) = 1 - \frac{1}{s(\alpha,L)}, \tag{2.3}$$

where $s(\alpha,L)$ is the average avalanche size of the system. For a critical process $s(\alpha,L)$ always increases with system size since there is no characteristic scale in the system. Thus in an infinitely large system a critical process is identified by $\sigma = 1$, while $\sigma < 1$ indicates a noncritical process. Recently, de Carvalho and Prado [11] calculated the system branching rate $\sigma(\alpha,L)$ for a range of different L values and inferred the infinite-size limit via extrapolation. Using this approach, they suggest that the OFC model has a branching rate smaller than 1 whenever $\alpha < 0.25$, with the branching rate close but not equal to 1 when α is close to the conservative limit $\alpha = 0.25$. This latter behavior has been termed ''almost critical'' and explains why the probability density plots appear linear [15]. These findings have remained controversial with alternative extrapolation procedures showing the results may be consistent with $\alpha_c^{\mathrm{NN}} \leqslant 0.23$ [14]. As a result the question of whether conservation is necessary for criticality in the OFC model remains open. We address precisely this issue in the next section.

III. THE LAYER BRANCHING RATE AND CRITICALITY

In order to infer information about how the OFC model behaves on arbitrarily large lattices, using simulation studies, it is necessary to introduce some form of extrapolation. Implicit in this approach is the assumption that near the center

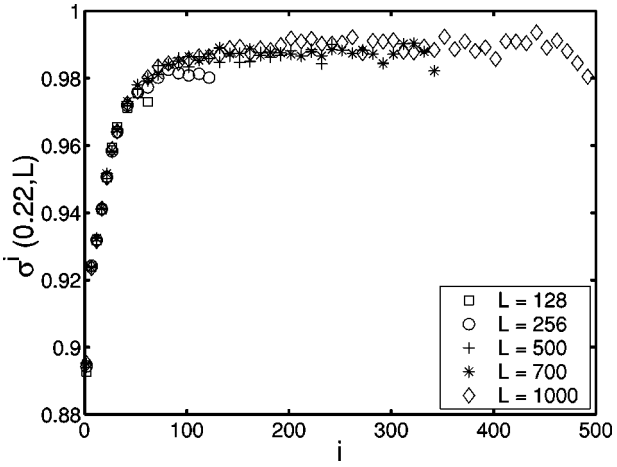

FIG. 1. The layer branching rate $\sigma^i(\alpha,L)$ for the nearest-neighbor OFC model calculated for the case $\alpha=0.22$ and a range of lattice sizes $L=128,256,500,700,1000$.

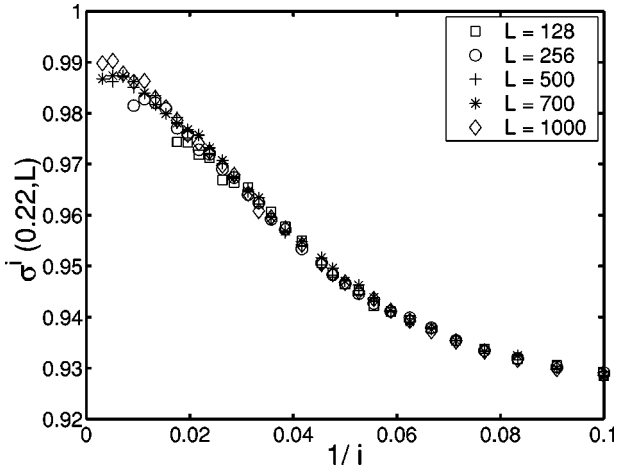

FIG. 2. The layer branching rate $\sigma^i(\alpha,L)$ for the nearest-neighbor OFC model calculated for the case $\alpha=0.22$ and a range of lattice sizes $L=128,256,500,700,1000$, plotted as a function of $1/i$.

of a large lattice the behavior approaches that of an infinitely large system. If this is the case we believe that more precise information can be extracted from the finite $(L\times L)$ simulations by calculating the *layer branching rates* $\sigma^i(\alpha,L)$, $i=1,\ldots,L/2$, for the lattice [throughout our study we assume that L is even; for L odd the $L/2$ here and below should be replaced by $(L+1)/2$]. Here σ^i measures the average number of descendants originating from a supercritical site that topples in layer i, where layer 1 contains all the sites on the boundary, layer 2 contains all sites one layer in from the boundary, and so on. Assuming that the sites farthest away from the boundaries do indeed behave more like those embedded in an infinitely large system, then for sufficiently large L, the σ^i will converge as i increases, with a plausible definition of the genuine branching rate $\sigma(\alpha)$ being given by

$$\sigma(\alpha)=\lim_{L\to\infty}\lim_{i\to L/2}\sigma^i(\alpha,L). \tag{3.1}$$

Since we are relying on simulation studies the first limit cannot be performed rigorously and so some form of extrapolation will still be required to deduce $\sigma(\alpha)$. However, one hopes that the influence of the boundaries on $\sigma^i(\alpha,L)$ will be small for i near $L/2$ in a large lattice. Thus the extrapolation should allow more accurate results for a given maximum system size L than direct examination of the branching rate $\sigma(\alpha,L)$, which does depend on the behavior near the boundary of the lattice.

A plot of some layer values $\sigma^i(\alpha,L)$ for the case $\alpha=0.22$ and a range of lattice sizes L is shown in Fig. 1. We note that the plots for the various system sizes do overlay one another for small layer numbers i, provided L is sufficiently large. More precisely, for a particular layer branching rate the simulation results converge as L increases with

$$\lim_{L\to\infty}\sigma^i(\alpha,L)=\sigma^i(\alpha), \tag{3.2}$$

where $\sigma^i(\alpha)$ is the value of the ith layer branching rate in an arbitrarily large system. We observe from our simulation results that, for fixed L, $\sigma^{L/2}(\alpha,L)$ is a poor guide to $\sigma^{L/2}(\alpha)$. Further, as the layer branching rates $\sigma^i(\alpha)$ for small enough values of i are easily accessible from the finite-size simulations it is profitable to replace Eq. (3.1) with

$$\sigma(\alpha)=\lim_{i\to\infty}\sigma^i(\alpha) \tag{3.3}$$

as our definition of the true system branching rate. While Fig. 1 allows us to identify a lower bound for $\sigma(\alpha)$ it does not enable easy extrapolation to the infinite-size limit. In Fig. 2 we plot the same layer branching rate data against the inverse of the layer number $1/i$. In this representation the results for the various lattice sizes can be straightforwardly extrapolated. In particular, for $i\geqslant 25$ the limiting values of the layer branching rate $\sigma^i(\alpha)$ lie on an approximately straight line which extrapolates to 0.996 ± 0.001. Thus we conclude $\sigma(0.22)\approx 0.996$ and so the OFC model is noncritical for this value of α. For clarity in Fig. 2 only a limited number of layer values have been plotted and a relatively large $1/i$ range has been used. It may not be clear from this figure that the limiting value of the layer branching rate could not be 1, and hence in Fig. 3 we show the results for the largest lattice size $(L=1000)$ on a larger scale, for which the extrapolation to a noncritical value is more apparent.

The general behavior described above for the case $\alpha=0.22$ is repeated for values of the conservation parameter $\alpha\leqslant 0.23$. Our results for the extrapolated branching rate and the corresponding prediction for the average avalanche size in the infinite volume limit $\langle s(\alpha)\rangle_\infty$ [found using Eq. (2.3)] are given in Table I. However, when α is close or equal to the conservative limit $\alpha=0.25$ the behavior is slightly more complicated. Thus before discussing the results further we first provide a more detailed description of the cases $\alpha=0.25$ and $\alpha=0.24$.

First, when $\alpha=0.25$ we find that the layer branching rates $\sigma^i(0.25)$ lie below 1 for the outer layers of the lattices, but $\sigma^i(0.25)\geqslant 1$ for $i\geqslant 5$. This behavior is shown in Fig. 4, which also shows that the layer branching rate converges

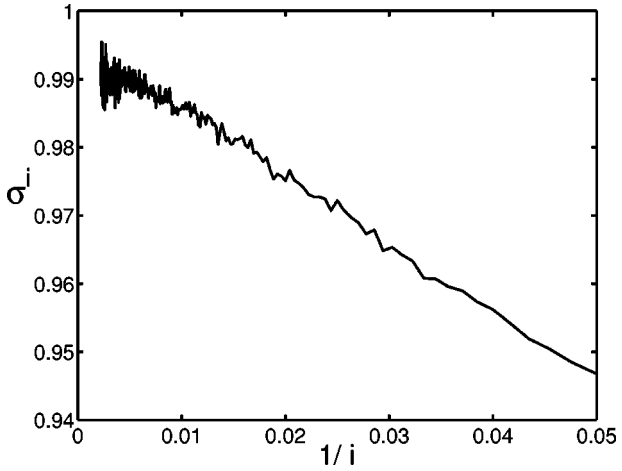

FIG. 3. The layer branching rate $\sigma^i(\alpha=0.22,L=1000)$ for the nearest-neighbor OFC model, plotted as a function of $1/i$.

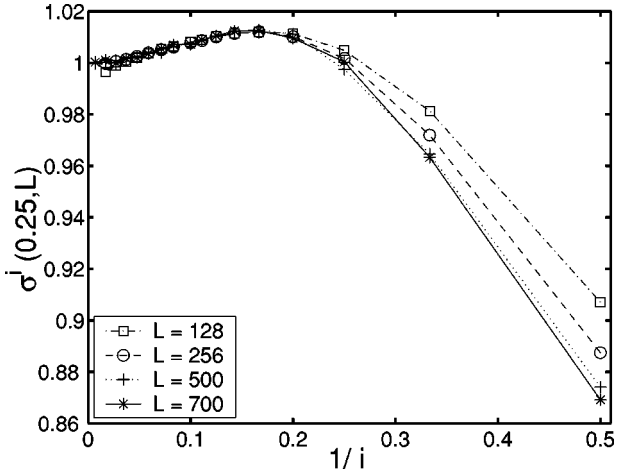

FIG. 4. The layer branching rate $\sigma^i(\alpha,L)$ for the nearest-neighbor OFC model calculated for the case $\alpha=0.25$ and a range of lattice sizes $L=128,256,500,700$, plotted as a function of $1/i$.

much more slowly in the outer layers in this case than for all other choices of α. In our simulations on smaller lattice sizes the layer branching rates dip below 1 again near the center of the lattice; however, this appears to be a finite-size result with the $i\to\infty$ limiting behavior, as the lattice size increases, tending toward 1 from above. As a result of this behavior the system branching rate for a finite lattice, $\sigma(0.25,L)$, as calculated by de Carvalho and Prado [11] is very sensitive to the definition of branching rate in the outermost layer. This explains why those authors found a value of the branching rate slightly larger than 1 for $\alpha=0.25$, which has been criticized for violating Eq. (2.3). This result is due to a weighting of the branching rate in the outside layer intended to account for the reduced number of neighbors present. Similarly, ignoring the outside layer entirely also leads to values of the branching rate larger than 1 in a finite simulation [11], since this essentially assumes that the branching rate of the outermost value takes the average value of the inner layers—it is clear from our study that this is not the case. In particular, we find $\sigma^1(\alpha=0.25)\approx 0.48$ in the unweighted case, $\sigma^1(\alpha=0.25)\approx 0.64$ in the weighted case, and $\sigma^1(\alpha=0.25)\approx 1$ if we use the average of the remaining inner layers.

When $\alpha=0.24$ the behavior is different again. The outer layers are reminiscent of the conservative case with the layer branching rates increasing to a value above 1 by the fifth layer. However, these supercritical values only persist up to around the 20th layer, after which the layer branching rate drops below 1, as shown in Fig. 5. Extrapolating the branching rate to the infinite-size limit again yields a value close to, but measurably below, 1, describing a noncritical system.

The various behaviors described above appear to indicate a continuously changing influence of the layers nearest the edges of the lattice as α is reduced from the conservative limit. For a typical α value the layer branching rates increase for the first few layers, reaching a (local) maximum within the outer five layers. As we go further into the interior of the lattice $\sigma^i(\alpha)$ decreases to a local minimum value before increasing again toward the limiting value $\sigma(\alpha)$. The location of the minimum provides a measure of the region of influ-

TABLE I. Values of the extrapolated system branching rate $\sigma(\alpha)$ and the corresponding extrapolated average avalanche size $\langle s(\alpha)\rangle_\infty$ for different values of the conservation parameter α. For $\langle s(\alpha)\rangle_\infty$ the ranges of possible values consistent with $\sigma(\alpha)$ are also shown. The largest lattice size considered is $L=1000$ except for $\alpha=0.25$ where only systems up to $L=700$ have been simulated.

α	$\sigma(\alpha)$	$\langle s(\alpha)\rangle_\infty$
0.17	0.940 ± 0.005	16.7 (15.4→18.2)
0.18	0.958 ± 0.005	23.8 (21.3→27.0)
0.19	0.979 ± 0.004	47.6 (40.0→58.8)
0.20	0.988 ± 0.003	83.3 (66.7→111)
0.21	0.9924 ± 0.0008	132 (119→147)
0.22	0.9958 ± 0.0008	238 (200→294)
0.23	0.9973 ± 0.0005	370 (313→455)
0.24	0.9987 ± 0.0005	769 (556→1250)
0.25	1.0000 ± 0.000006	∞ (166667→∞)

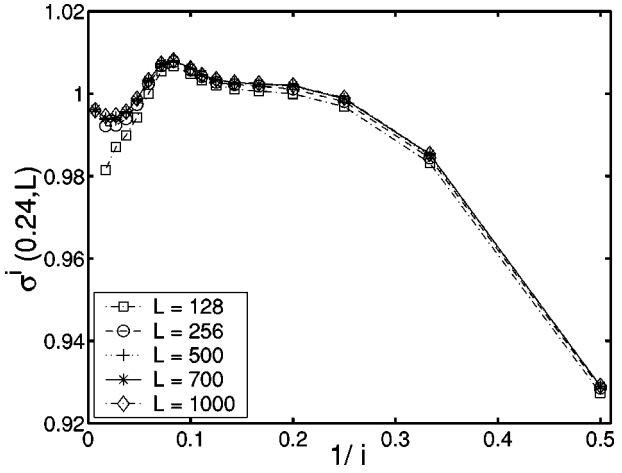

FIG. 5. The layer branching rate $\sigma^i(\alpha,L)$ for the nearest-neighbor OFC model calculated for the case $\alpha=0.24$ and a range of lattice sizes $L=128,256,500,700,1000$, plotted as a function of $1/i$.

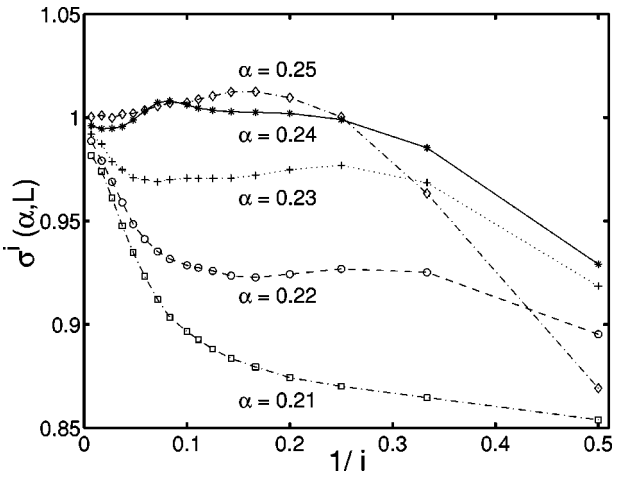

FIG. 6. The layer branching rate $\sigma^i(\alpha,L)$ for the nearest-neighbor OFC model calculated for a range of conservation values $\alpha=0.21,0.22,0.23,0.24,0.25$, plotted as a function of $1/i$. For $\alpha=0.25$ a lattice of size $L=700$ has been used, while $L=1000$ for all other values of α shown.

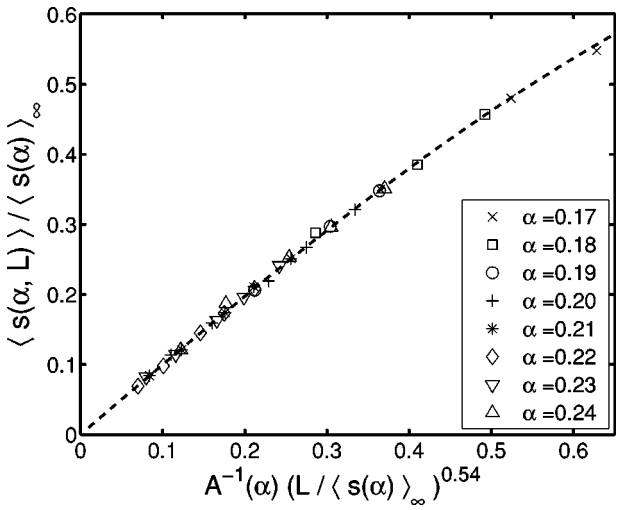

FIG. 7. The scaled average avalanche size $\langle s(\alpha,L)\rangle/\langle s(\alpha)\rangle_\infty$ plotted for a range of α and L values. The dashed line is the tanh fit given in Eq. (3.4).

ence of the enhanced values near the edge of the lattice. The results for a range of α values are shown in Fig. 6. For $\alpha=0.25$ the minimum is only reached in the infinite size limit, with the enhanced values persisting for all of the interior layers, leading to criticality. When $\alpha=0.24$ we have seen (Fig. 5) that the maximum takes a supercritical value, and the minimum is not reached until one is at least 50 layers into the system. Thus, if we interpret the location of the minimum as a guide to the extent of finite-size effects in a noncritical system, we see that large lattices need to be simulated to overcome these effects when $\alpha=0.24$. For $\alpha=0.23$ the local maximum near the boundary is no longer the global maximum, and the minimum is reached within the first 25 layers. As α is further decreased the local maximum and minimum approach one another, and by the time $\alpha=0.21$ they have disappeared altogether, with the layer branching rates displaying monotonic behavior. Finally, we note that for any $\alpha_1<\alpha_2<0.25$ one finds $\sigma^i(\alpha_1)<\sigma^i(\alpha_2)$ for all layers i, while the results for $\alpha=0.25$ clearly do not satisfy this relationship (see Fig. 6).

Our results for the system branching rate $\sigma(\alpha)$ given in Table I are considerably larger than the values quoted by de Carvalho and Prado [11], indicating that the systems are nearer criticality than previously predicted. We believe our results are more accurate because we have used the individual layer branching rates, rather than the finite-system branching rate $\sigma(\alpha,L)$, which is strongly affected by the results in the outermost layers. For example de Carvalho and Prado find $\sigma(\alpha=0.22,L)\approx 0.955$ for the largest lattice they consider, which is a reasonable measure of the average branching rate across a finite number of layers. However, comparison with Fig. 2 shows that this estimate is significantly lower than the layer branching rate for all but the 50 outermost layers of any simulation. Despite these quantitative differences our results do agree qualitatively, with critical behavior in the nearest-neighbor OFC model being predicted only in the conservative limit $\alpha=0.25$.

Further support for this prediction can be found from the average avalanche sizes $\langle s(\alpha,L)\rangle$ determined for various conservation levels α and lattice sizes L. For fixed $\alpha<0.25$ and $L\leqslant 500$ we find that $\langle s(\alpha,L)\rangle$ scales like $\langle s(\alpha,L)\rangle\sim L^{0.54}$. Although $\langle s(\alpha,L)\rangle$ increases rapidly with L for relatively small lattice sizes, we assume that as $L\to\infty$ one finds $\langle s(\alpha,L)\rangle\to\langle s(\alpha)\rangle_\infty$ suggesting that a tanh function might yield a sensible fit for noncritical choices of α. In particular, we have fitted our data using

$$\frac{\langle s(\alpha,L)\rangle}{\langle s(\alpha)\rangle_\infty}=\tanh\left(\frac{1}{A(\alpha)}\left[\frac{L}{\langle s(\alpha)\rangle_\infty}\right]^{0.54}\right), \qquad (3.4)$$

where $A(\alpha)$ and $\langle s(\alpha)\rangle_\infty$ are used as fitting parameters. The fact that L and $\langle s(\alpha)\rangle_\infty$ scale together inside the tanh function initially seems counterintuitive. However, observation of the sites involved in a given avalanche on the computer screen reveals that a typical avalanche of size n_s involves sites in a long thin chain (with length of order n_s) rather than a "blob" with radius of order $\sqrt{n_s}$, as might be anticipated. We find that Eq. (3.4) provides an excellent fit for all $\alpha\leqslant 0.24$ as shown in Fig. 7. The values of the fitting parameters are give in Table II. The function $A(\alpha)$ is approximately constant for $\alpha<0.22$ and vanishes like $(1-4\alpha)$ as $\alpha\to 0.25$. The values of $\langle s(\alpha)\rangle_\infty$ compare favorably with those given in Table I which were estimated directly from the branching rate data. Thus predictions of the branching rate found from assuming the fitting function are also in good agreement with those found by direct measurement. For $\alpha=0.25$ the data for $\langle s(\alpha,L)\rangle$ follow a completely different

TABLE II. Values of the fitting parameters $A(\alpha)$ and $\langle s(\alpha)\rangle_\infty$ used in Fig. 7.

α	0.17	0.18	0.19	0.20	0.21	0.22	0.23	0.24
$A(\alpha)$	11.60	11.60	11.60	11.60	11.30	10.20	7.10	3.28
$\langle s(\alpha)\rangle_\infty$	17.7	27.8	48.5	81.6	140	240	368	700

pattern, always displaying an algebraic growth with L, which is well modeled by the approximation $\langle s(\alpha,L)\rangle \approx L^{2.4}/43$. Hence, while we accept that Eq. (3.4) may only be one of many fits for the limited amount of data presented, it does demonstrate a level of universality in the avalanche size data for the nonconservative choices of α, which is absent in the conservative case $\alpha=0.25$. This provides further evidence that criticality is found only in the conservative case.

In conclusion, in this section we have analyzed simulation data for both layer branching rates and average avalanche sizes. All of these data are consistent with the prediction that the nearest-neighbor OFC model is critical only in the limit $\alpha=0.25$. However, our predictions for the system branching rates are generally higher than previously suggested, indicating that the model is ''almost critical'' for a wide range of α values.

IV. ORGANIZATION IN RANDOM- AND NEAREST-NEIGHBOR OFC MODELS

In this section we present some analytic results describing control cases for the OFC models. The aim of this section is to determine how well the OFC models organize themselves toward criticality, regardless of whether they are genuinely critical or not. To determine this we consider control models in which the data are *not organized* and calculate the branching rate to compare with those of the full random-neighbor and nearest-neighbor OFC models. Thus, in our control cases we assume that the site energies u_{ij} at the start of each avalanche are drawn from a uniform distribution in the range $[0,1)$. We consider the RN and NN cases in turn below.

A. Random-neighbor model

To begin we analyze the random-neighbor OFC model for which some useful results can be found in the literature. In particular, we reconsider the paper by Lise and Jensen [12] that initiated analytic investigation of the random neighbor OFC model as discussed in Sec. II. Although their original study was intended to describe the full RN OFC model, many of the simplifications that LJ used are actually more appropriate for our control case study. Most notably, they assumed that the distribution of energies in subcritical sites follow a uniform distribution at every stage of the avalanche. Using this assumption they identified that the branching rate σ is given exactly by

$$\sigma = 4\alpha\langle E^+\rangle, \tag{4.1}$$

where $\langle E^+\rangle$ is the average energy of a supercritical site immediately prior to toppling. Within their analysis LJ estimated $\langle E^+\rangle$ by assuming that the statistics of ancestor and descendant sites are the same. To clarify, let us denote the first site in the avalanche to topple as being generation 0, all supercritical sites directly generated by this topple as generation 1, all supercritical sites resulting from generation 1 topples as generation 2, and so on. Using this definition LJ assumed that for any two generations i and j, $\langle E_i^+\rangle = \langle E_j^+\rangle$, where $\langle E_i^+\rangle$ is the average energy of a supercritical site in generation i. We believe this assumption is acceptable for identifying the crossover value α_c (which was the purpose of the LJ study) but is not suitable in general. To see why this is the case, we note that if $\langle n_i\rangle$ represents the average number of supercritical sites in generation i then $\langle E^+\rangle$ is formally given by

$$\langle E^+\rangle = \frac{\sum_{i=0}^{\infty}\langle n_i\rangle\langle E_i^+\rangle}{\sum_{i=0}^{\infty}\langle n_i\rangle}. \tag{4.2}$$

For a critical process these summations are dominated by contributions from high generations (large i). In this case $\langle E_i^+\rangle$ approaches a limiting value [identified by LJ as $1/(1-\alpha/2)$] which is an excellent approximation for $\langle E^+\rangle$. However, for a noncritical process a typical avalanche only lasts a small, finite number of generations and so the summations in Eq. (4.2) are dominated by low generation numbers. As we show below the assumption $\langle E_i^+\rangle = \langle E_j^+\rangle$ is not accurate for early generations and hence the LJ calculation needs to be revised.

Now we are in a position to consider our control case for the RN OFC model. Within this model we use the same toppling algorithm for distributing the energy to neighboring sites as in the full RN OFC model. Here we model an infinitely large system in which we assume that no site receives more than one contribution in a single avalanche; hence the energy distribution of receiving sites is always uniform. This factor stops any organization of the system, yielding the branching rate of a nonorganized system. As the control model uses uniform data at the start of each avalanche it is reasonable to try to obtain analytic results.

We start by looking at the energy distributions of supercritical sites in each generation. We denote the normalized distribution at generation j by $f_j(1+k)$ where $(1+k)$ is the supercritical energy value. For a specific generation $j \geqslant 1$ the possible energy values are found to satisfy $0 \leqslant k \leqslant g_j(\alpha)$ where $g_j(\alpha) = \Sigma_{i=1}^{j}\alpha^i$. Given the distribution function at generation j we can calculate $\langle E_j^+\rangle$ via the definition

$$\langle E_j^+\rangle = \int_0^{g_j(\alpha)} (1+k) f_j(1+k)\, dk. \tag{4.3}$$

As we are trying to model an infinitely large system we assume that prior to the start of an avalanche the site with maximum energy takes a value arbitrarily close to 1. Thus after the driving phase all other sites remain uniformly distributed in the range $(0,1)$. Hence the avalanche begins with a single seed site with an energy value identically equal to 1. This seed site is what we denote generation 0. The supercritical energy distribution of this zeroth generation is therefore given by a δ function located at 1, so $f_0 = \delta(1)$, $\langle E_0^+\rangle = 1$, and $\langle n_0\rangle = 1$. In toppling this site to four random neighbors we obtain the distribution for f_1, which is uniform in the range $(1,1+\alpha)$. More generally, we can relate f_j and f_{j+1} through

$$f_{j+1}(1+k')=\begin{cases}\dfrac{1}{\mathcal{N}}\displaystyle\int_{h(k',\alpha)}^{g_j(\alpha)} f_j(1+k)dk, & 0\leqslant k'\leqslant g_{j+1}(\alpha),\\ 0, \quad \text{otherwise,}\end{cases} \tag{4.4}$$

where $g_j(\alpha)$ is defined above, $h(k',\alpha)=\max[0,(1/\alpha)\times(k'-\alpha)]$, and the normalization factor $\mathcal{N}=\int_0^{g_{j+1}(\alpha)}\int_{h(k',\alpha)}^{g_j(\alpha)} f_j(1+k)dkdk'$.

Using Eqs. (4.3) and (4.4) recursively we can formally calculate $\langle E_j^+\rangle$ for any $j\geqslant 1$ using only our knowledge about the distribution f_1. In practice, we find that f_j is a piecewise defined function containing j nonzero pieces, and as a result for arbitrarily large j the iterative application of these equations becomes computationally prohibitive. However, worthwhile progress can still be made by noting that in addition to Eq. (4.3) we can also work out $\langle E_{j+1}^+\rangle$ using the distribution f_j. Specifically, for a supercritical site in generation j with energy $1+k$, a neighboring site will become supercritical at generation $j+1$ with probability $\alpha(1+k)$. The supercritical energy of this descendant site is uniformly distributed in the range $(1,1+\alpha+\alpha k)$; therefore the average value is $(1+\alpha/2+\alpha k/2)$. To determine $\langle E_{j+1}^+\rangle$ we must integrate over all the possible k values in the range $0\leqslant k\leqslant g_j(\alpha)$, where we need to weight each contribution of $(1+\alpha/2+\alpha k/2)$ by the appropriate ancestor probability $f_j(1+k)$ and descendant probability $\alpha(1+k)$, yielding

$$\langle E_{j+1}^+\rangle=\frac{\displaystyle\int_0^{g_j(\alpha)}(1+k)[1+(\alpha/2)(1+k)]f_j(1+k)dk}{\displaystyle\int_0^{g_j(\alpha)}(1+k)f_j(1+k)dk}. \tag{4.5}$$

Either Eq. (4.3) or Eq. (4.5) can be used to obtain (the same) results for the average supercritical energy in the first few generations:

$$\langle E_0^+\rangle=1, \tag{4.6}$$

$$\langle E_1^+\rangle=1+\frac{\alpha}{2}, \tag{4.7}$$

$$\langle E_2^+\rangle=1+\frac{\alpha}{2}+\frac{\alpha^2}{4}+\frac{\alpha^3}{24+12\alpha}. \tag{4.8}$$

For a given distribution function f_j we define the corresponding expectation operator $\mathbf{E}_j$ in a standard fashion with $\mathbf{E}_j[s(k)]=\int_0^{g_j(\alpha)}s(k)f_j(1+k)dk$. Thus Eq. (4.5) can be rewritten in the form

$$\langle E_{j+1}^+\rangle=1+\frac{\alpha}{2}\frac{\mathbf{E}_j[(1+k)^2]}{\mathbf{E}_j[(1+k)]}, \tag{4.9}$$

where by definition [see Eq. (4.3)]

$$\mathbf{E}_j[(1+k)]=\langle E_j^+\rangle. \tag{4.10}$$

Using this and the statistical definition of the variance, Eq. (4.9) simplifies to

$$\langle E_{j+1}^+\rangle=1+\frac{\alpha}{2}\langle E_j^+\rangle+\frac{\alpha}{2}\frac{\mathrm{Var}_j(1+k)}{\langle E_j^+\rangle}. \tag{4.11}$$

Although we cannot determine the value of $\mathrm{Var}_j(1+k)$ without finding $f_j(1+k)$, we do know it is non-negative. Hence by assuming that the contribution is zero we obtain a formal lower bound for $\langle E_{j+1}^+\rangle$ using only $\langle E_j^+\rangle$. Applying this method recursively, starting from $\langle E_0^+\rangle=1$ we find the lower bound $\langle E_1^+\rangle^<=1+\alpha/2$, which is identical to the exact result Eq. (4.7), while $\langle E_2^+\rangle^<=1+\alpha/2+\alpha^2/4$, which should be compared with Eq. (4.8). The general result is

$$\langle E_j^+\rangle^<=\sum_{i=0}^{j}\left(\frac{\alpha}{2}\right)^i, \tag{4.12}$$

which holds for any $j\geqslant 0$.

We can use these lower bounds in Eq. (4.2) to approximate $\langle E^+\rangle$ provided we find corresponding approximations for the average number of supercritical sites $\langle n_i\rangle$ in a given generation. The procedure for calculating $\langle n_{j+1}\rangle$ from $\langle n_j\rangle$ is similar to that used in finding Eq. (4.5). In particular, noting that $4\langle n_j\rangle$ sites receive contributions at this level, we obtain

$$\langle n_{j+1}\rangle=4\alpha\langle n_j\rangle\int_0^{g_j(\alpha)}(1+k)f_j(1+k)dk=4\alpha\langle n_j\rangle\langle E_j^+\rangle. \tag{4.13}$$

For the first few generations this gives $\langle n_0\rangle=1$, $\langle n_1\rangle=4\alpha$, and $\langle n_2\rangle=16\alpha^2(1+\alpha/2)$. Inserting Eq. (4.13) into Eq. (4.2) yields an exact expression for $\langle E^+\rangle$ in terms of the individual generation supercritical energies $\langle E_j^+\rangle$. If we let $\langle E^+\rangle^{(p)}$ represent the approximation to $\langle E^+\rangle$ found by truncating the summations in Eq. (4.2) at generation p, we find

$$\langle E^+\rangle^{(p)}=\frac{\displaystyle\sum_{i=0}^{p}\left\{(4\alpha)^i\prod_{j=0}^{i}\langle E_j^+\rangle\right\}}{1+\displaystyle\sum_{i=0}^{p-1}\left\{(4\alpha)^{i+1}\prod_{j=0}^{i}\langle E_j^+\rangle\right\}}. \tag{4.14}$$

We approximate $\langle E_j^+\rangle$ using the lower bounds given in Eq. (4.12) to obtain approximate values for $\langle E^+\rangle^{(p)}$ for a range of p values. As p gets large the error due to truncation is reduced, and we formally obtain our approximation for $\langle E^+\rangle$ by considering the limit $p\to\infty$. We have compared our predictions with simulations of the control model and the results are shown in Fig. 8, where for comparison we have also plotted the LJ approximation $\langle E^+\rangle^{\mathrm{LJ}}=1/(1-\alpha/2)$ [12]. We can see that, although our result is approximate, because we have used the lower bounds $\langle E_j^+\rangle^<$, it is in excellent agreement with the simulation data. The LJ results are significantly larger until $\alpha=2/9$, after which our results coincide because the control model becomes critical (see below), and as discussed earlier the LJ approximation is a reasonable one for cases where the model is critical.

The goal of this section is to calculate the branching rate σ for the control model. Since the distribution of subcritical

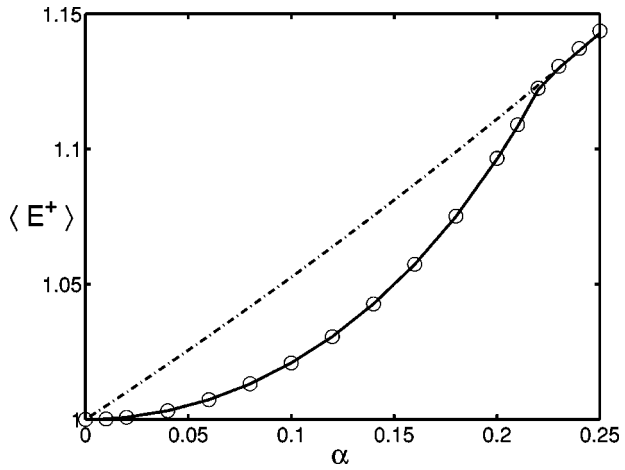

FIG. 8. Average toppling energies $\langle E^+\rangle$ calculated for the random neighbor control model via simulations (circles) and approximated using lower bounds $\langle E_j^+\rangle^<$ for the generation toppling energies (solid line). The result of the Lise-Jensen approximation method is also shown (dot-dashed line).

sites has been assumed uniform in the range (0,1), Eq. (4.1) can be used to find σ. Within our scheme we use our approximation for $\langle E^+\rangle$ to derive a value for the branching rate which is again found to be in excellent agreement with the simulation results of the control case. Thus we believe our results can be used to provide a reliable measure of the organizational quality of the full RN OFC model. As expected, we find that the control model is critical ($\sigma \geqslant 1$) when $\alpha \geqslant 2/9$, in agreement with the analysis of LJ [12]. In Fig. 9 we plot the branching rates for the control case and the full model. We note from this figure that the branching rate in the full model for all α values is lower than in the control case; this indicates that organization in the RN model is a negative feature. In other words, the organized data are less critical than uniformly random data.

Hence, in conclusion, we believe that the random-neighbor OFC model is a poor prototype for studying self-organized criticality in two respects. First, as has previously been established it is always noncritical in the nonconservative regime. Secondly, we have shown here that the organizational process in the RN OFC model lowers the level of criticality in comparison with uniform random data.

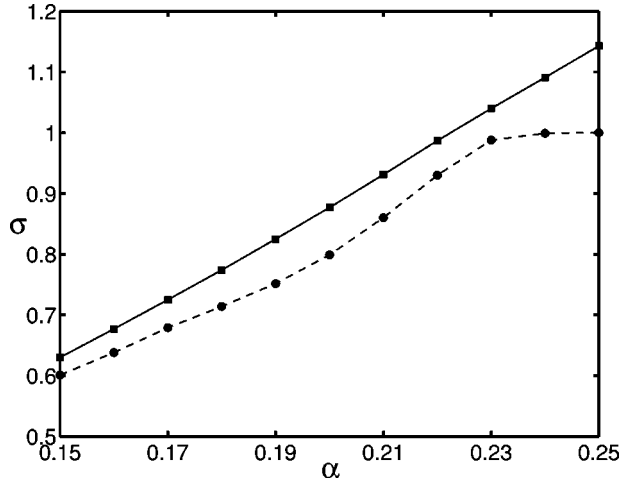

FIG. 9. Branching rate for the full random-neighbor OFC model (dashed) and the control case (solid) plotted as a function of the conservation parameter α.

B. Nearest-neighbor model

We now examine a similar control model for a nearest-neighbor situation. At the start of each avalanche the energies of noncritical sites are again assumed to be distributed uniformly in [0,1). In contrast to the random-neighbor study above, we no longer expect this simplification to allow us to develop a complete theory as correlations are expected to build up during the course of a single avalanche. This follows since sites may receive contributions from more than one neighbor, and topple more than once during a given avalanche. Thus we will need to rely on simulations of the control model to some extent. However, we examine the first few generations of the toppling process analytically in a similar fashion as in Sec. IV A in order to identify how the NN control model deviates from its RN counterpart. The theory will also provide an independent test of the simulation results.

The control model starts as for the RN case with generations 0 and 1 being identical. We can still apply Eq. (4.3) in calculating $\langle E_j^+\rangle$ provided the upper limit on the integral is appropriately modified (for simplicity we set it to ∞, for which the equation is always valid). Generation 2 is more complicated than for the RN case since, as mentioned above, we have to take into account that a second generation site can receive contributions from two neighboring first generation supercritical sites. In generation 1 there can be zero to four supercritical sites; to analyze generation 2 we have examined each of these possibilities in turn, weighting the cases appropriately. The calculation is further complicated by the observation that the seed site (generation 0 toppling site) can become supercritical again in generation 2 if all four sites in generation 1 are supercritical and $\alpha \geqslant (\sqrt{2}-1)/2$. For simplicity at this stage we exclude this possibility but we provide a quantitative measure of its significance below.

Our expressions for $\langle E_2^+\rangle$ and $\langle n_2\rangle$ are

$$\langle E_2^+\rangle = 1 + \frac{\alpha}{2} + \frac{7\alpha^2 + 6\alpha^3 + \alpha^4}{12 + 6\alpha}, \tag{4.15}$$

and

$$\langle n_2\rangle = 6\alpha^2(2+\alpha). \tag{4.16}$$

The supercritical energy $\langle E_2^+\rangle$ is larger than the corresponding RN result, $\langle E_2^+\rangle^{\mathrm{RN}} = 1 + \alpha/2 + (3\alpha^2 + 2\alpha^3)/(12 + 6\alpha)$ [see Eq. (4.8)], which is precisely due to the possibility of sites receiving contributions from more than one generation 1 neighbor. This apparent aid to criticality is negated by a reduced number of generation 2 supercritical sites $\langle n_2\rangle$, which is only 3/4 of the value found in the RN case [see after Eq. (4.13)]. We again let $\langle E^+\rangle^{(p)}$ represent the approximation to $\langle E^+\rangle$ found by truncating the summations in Eq. (4.2) at generation p. Our results for $p = 0,1,2$ are shown in Fig. 10

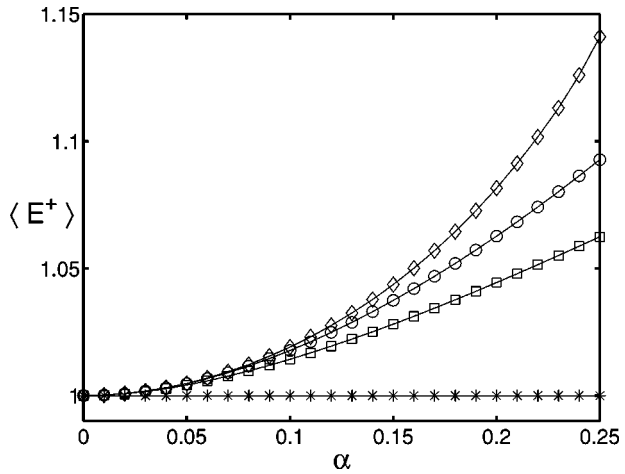

FIG. 10. Average toppling energy $\langle E^+ \rangle$ for the nearest-neighbor control model determined using simulations (diamonds), and the corresponding approximations $\langle E^+ \rangle^{(p)}$ for $p=0$ (stars), $p=1$ (squares), and $p=2$ (circles).

along with simulation results for the full $\langle E^+ \rangle$. Due to the spatial organization in the NN model one can no longer use Eq. (4.1) for determining the branching rate σ. However, we can use our results for the first few generations to calculate approximations for σ. Truncating after generation 1 gives $\sigma^{(1)}=4\alpha$, while truncating after generation 2 yields $\sigma^{(2)}=(4\alpha+12\alpha^2+6\alpha^3)/(1+4\alpha)$. By generation 2 the branching rate in the NN control model is below that in the corresponding RN case, a feature that is also found in simulations of the two models. This difference is directly attributable to the reduced number of supercritical sites $\langle n_2 \rangle$ in generation 2. Both $\langle E^+ \rangle^{(2)}$ and $\sigma^{(2)}$ prove to be excellent approximations for $\alpha \leqslant 0.1$, but as can be seen from Fig. 10 more generations are clearly required for larger α. Since the control model is only being used to test the effect of organization in the full NN OFC model we do not believe that analytic examination of further generations is justified given the effort required.

Before turning to the issue of organization we briefly comment on the effect of including the possible retopple of the seed site, mentioned above, upon our results. We concentrate on the case $\alpha=0.25$ for which this retopple is most likely to occur, and hence has the greatest impact. We find that $\langle E^+ \rangle^{(2)}$ changes from 1.092 806 to 1.092 850 and $\sigma^{(2)}$ changes from 0.9219 to 0.9297 upon including the retopple, so that in each case the change is less than 1%. Finally, in Fig. 11 we show the normalized energy distribution functions for generations 1 and 2 for the case $\alpha=0.25$. For generation 2 we have included the retoppling of the seed site, which directly leads to the bump in the distribution between 1 and $1+\alpha=1.25$. In the absence of the seed site retopple the distribution function is flat in this region but is otherwise indistinguishable from that shown in Fig. 11.

To conclude this section we want to compare the branching rate of our unorganized control model with the full NN OFC model results found in Sec. III. The two sets of results are shown in Fig. 12 which reveals that the NN OFC model generally has a much higher branching rate than the control case. This contrasts strongly with the RN situation (see Fig. 9) and leads us to conclude that organization in the nearest-neighbor OFC model is a positive feature. To get a quantitative measure of the quality of the organizational process we introduce the *organization parameter* μ via

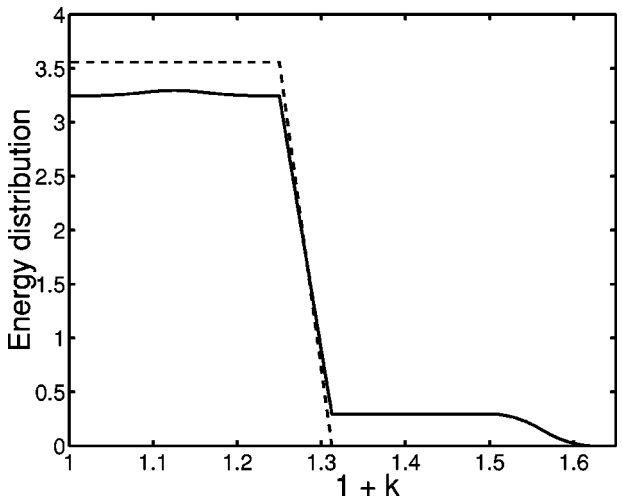

FIG. 11. Normalized energy distribution functions of supercritical sites in generation 1 ($f_1(1+k)$, dashed), and generation 2 ($f_2(1+k)$, solid) of the nearest-neighbor control model, plotted as functions of the energy $E=1+k$.

$$\mu = \frac{\sigma - \sigma^{\text{control}}}{1 - \sigma^{\text{control}}}, \tag{4.17}$$

where σ and σ^{control} are the branching rates in the full OFC model and control model, respectively. With this definition μ measures proportionally how much closer the NN OFC model is to criticality compared to the control model. Thus $\mu=0$ indicates that the organized data are no more critical than uniformly random data, and $\mu=1$ implies that the organized system is critical with $\sigma=1$. Results for μ for a range of α values are shown in Table III, where our data for σ^{control} are also given. To calculate μ we have used the σ

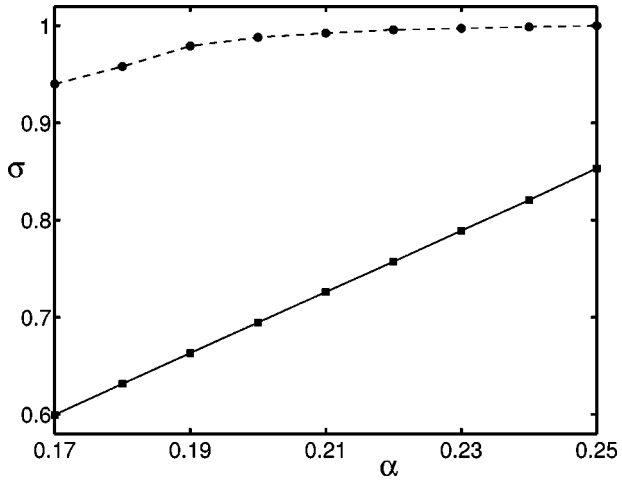

FIG. 12. Branching rate for the full nearest-neighbor OFC model (dashed) and the control case (solid) plotted as a function of the conservation parameter α.

TABLE III. Values of the nearest-neighbor control model branching rate σ^{control} and the organization parameter μ for different choices of the conservation parameter α.

α	σ^{control}	μ
0.17	0.5995	0.850 ± 0.013
0.18	0.6315	0.886 ± 0.014
0.19	0.6631	0.938 ± 0.012
0.20	0.6946	0.961 ± 0.010
0.21	0.7259	0.972 ± 0.003
0.22	0.7572	0.983 ± 0.003
0.23	0.7890	0.987 ± 0.003
0.24	0.8205	0.993 ± 0.003
0.25	0.8533	1.000 ± 0.00005

data from Table I, which also leads to the error estimates shown. These results show that self-organization in the nearest-neighbor OFC model takes the system at least 95% of the way toward criticality whenever $\alpha \geqslant 0.20$. Thus, although we do not believe the model is genuinely critical in the nonconservative regime $\alpha < 0.25$, it does do a good job of organizing toward a critical state.

In this section we have examined organization within the nearest- and random-neighbor OFC models and found that this is very good in the NN case, but is poor in the RN case. This suggests that spatial correlations are essential for good organization. In the RN OFC model spatial correlations cannot exist, and although the model does organize itself the resulting system is less critical than uniformly random data. In the NN OFC model spatial correlations are strong and enable the system to approach a nearly critical state for a wide range of α values.

V. SUMMARY AND CONCLUSIONS

The OFC model is one of the most widely studied prototypes for self-organized criticality. In this paper we have examined both the level of criticality and the quality of self-organization that the model possesses. By introducing layer branching rates and using extensive simulation studies we have established that the nearest-neighbor OFC model is only critical in the conservative limit $\alpha = 0.25$. A similar result is known to hold for the random-neighbor OFC model, suggesting that conservation is an essential ingredient in obtaining a critical system. Our results are based on simulation studies of finite-sized lattices and so one could argue that criticality would be observed if larger systems were studied. Such a criticism always applies to simulation studies; however, we note that the layer branching rates near the center of the large lattices fall convincingly on approximately straight lines which do not extrapolate to $\sigma = 1$ and thus we are confident that the model is not critical in the nonconservative regime.

In order to examine the organization process we have introduced control models for both random- and nearest-neighbor cases. These models use unorganized uniform random data for the energies at the start of each avalanche. By comparing the branching rate of the control models to those of the full OFC models we have shown that organization lowers criticality in the random-neighbor case. In contrast, self-organization greatly increases criticality in the nearest-neighbor case, yielding nearly critical systems for $\alpha \geqslant 0.20$.

Thus in the nonconservative regime we conclude that the random-neighbor OFC model is poor, being neither critical nor better organized than uniform random data. The nearest-neighbor OFC model also fails to be critical in the nonconservative regime, but the organization in this model is good leading to branching rates close to 1. Indeed, our estimates of the branching rate in the model are considerably higher than previous predictions, and as a result this model may provide the intended explanation of the ubiquity of power law distributions in nature. For the branching rates found we would expect to observe behavior consistent with a power law over the large but finite range that would be observable in an experimental system. Hence, we have shown that self-organized ''almost criticality'' is a robust phenomenon in the nearest-neighbor OFC model and would provide a plausible explanation of many power law observations in nature.

ACKNOWLEDGMENT

This research was supported in part by The Royal Society, U.K.

[1] An excellent review of the field is provided by H.J. Jensen, *Self-Organized Criticality* (Cambridge University Press, Cambridge, England, 1998).
[2] An accessible introduction to the subject is given by P. Bak, *How Nature Works* (Oxford University Press, Oxford, 1997).
[3] P. Bak, C. Tang, and K. Wiesenfeld, Phys. Rev. Lett. **59**, 381 (1987); Phys. Rev. A **38**, 364 (1988).
[4] T. Hwa and M. Kardar, Phys. Rev. Lett. **62**, 1813 (1989); S.S. Manna, L.B. Kiss, and J. Kertész, J. Stat. Phys. **61**, 923 (1990).
[5] Z. Olami, H.J.S. Feder, and K. Christensen, Phys. Rev. Lett. **68**, 1244 (1992); K. Christensen and Z. Olami, Phys. Rev. A **46**, 1829 (1992).
[6] R. Burridge and L. Knopoff, Bull. Seismol. Soc. Am. **57**, 341 (1967).
[7] H.-M. Bröker and P. Grassberger, Phys. Rev. E **56**, 3944 (1997).
[8] M.-L. Chabanol and V. Hakim, Phys. Rev. E **56**, R2343 (1997).
[9] S.T.R. Pinho and C.P.C. Prado, Eur. Phys. J. B **18**, 479 (2000).
[10] P. Grassberger, Phys. Rev. E **49**, 2436 (1994).
[11] J.X. de Carvalho and P.C. Prado, Phys. Rev. Lett. **84**, 4006 (2000); **87**, 039802 (2001).
[12] S. Lise and H.J. Jensen, Phys. Rev. Lett. **76**, 2326 (1996).
[13] S.T.R. Pinho, C.P.C. Prado, and O. Kinouchi, Physica A **257**, 488 (1998).
[14] K. Christensen, D. Hamon, H.J. Jensen, and S. Lise, Phys. Rev. Lett. **87**, 039801 (2001).
[15] O. Kinouchi and C.P.C. Prado, Phys. Rev. E **59**, 4964 (1999).